Chapter 6

Corrosion Protection of Magnesium Alloys: From Chromium VI Process to Alternative Coatings Technologies

Jérôme Frayret, Jean Charles Dupin and Sébastien Pommiers

Additional information is available at the end of the chapter

http://dx.doi.org/10.5772/66604

Abstract

Magnesium and its alloys present several advantages such as a high strength/weight ratio and a low density. These properties allow them to be used for many aeronautical applications but they are very sensitive to corrosion. In order to solve this problem, chromium VI conversion coatings (CCC) are deposited on the surface before a protective top coat application. This process is now limited by several environmental laws due to the high toxicity of hexavalent chromium. However the chemical mechanisms of CCC deposition will be detailed in this chapter in order to understand the chemical properties of this coating. Pre-treatment steps allow cleaning and preparing the surface for improving the coating deposition. A final layer of chromium (III) oxide and magnesium hydroxide composes the coating allowing the protective properties. Orthorhombic potassium chromate clusters trapped on the coating surface give self-healing property to the coating. Alternative conversion coatings are based onto solutions containing chromium (III), permanganate, phosphates, Rare Earth Elements (REEs) or vanadium. The second part of this chapter will detail the deposition and the protection mechanisms of these promising processes of CrVI substitution. Among them, permanganate/phosphate-based coating presents a better corrosion resistance than CCC and REEs have very efficient self-healing properties.

Keywords: corrosion protection, magnesium, alternative coatings, chromium VI, electrochemistry, surface analysis

1. Introduction

Magnesium alloys possess the lowest density of all metallic constructional materials and have good mechanical properties [1, 2]. They are suitable for the partial replacement of aluminium alloys for motorsport and aerospace applications. This could imply non-negligible weight and fuel savings in the aeronautical sector. Unfortunately, these materials are also very vulnerable to corrosion, do not resist wear and are highly chemically reactive [3]. Other metals, such as aluminium and lithium, have been added to pure magnesium to decrease its shortcomings [4], which limit the use of magnesium and its alloys for computer parts and in the aerospace and the automotive industries [5]. The poor corrosion resistance of magnesium is the consequence of its standard potential ($E°$ = −2.363 V/SHE (standard hydrogen electrode)), which makes it extremely susceptible to galvanic corrosion [5].

In order to decrease their corrosion sensitivity, several processes can be used to deposit a protective film on the surface of the alloy: anodizing, sol-gel process, gas-phase deposition process and chemical conversion [6]. Among these methods, chemical conversion is the least expensive and the easiest to perform [6, 7]. Protection is achieved by the immersion of the concerned substrate in pre-treatment and treatment baths. The classical pre-treatment process comprises a degreasing bath to clean the surface up [8] and several acidic baths to make the alloy rough and reactive enough before the coating deposition. Afterwards, the piece is immersed in the treatment bath for several minutes in order to deposit a protected coating on its surface. Until now, chromate conversion coatings (CCCs) have been widely used, despite the health concerns raised by the use of hexavalent chromium, because they offer the best protection against corrosion [9, 10]. The implementation, in June 2017, of the Regulation on Registration, Evaluation, Authorization and Restriction of Chemicals (REACH) will prohibit the use of such toxic compounds [11].

In the first part of this chapter, the chemical mechanism of chromate conversion is explored on magnesium alloy EV31A as it appears to be a key point in the protection process. Some assumptions suggested that polar oxo-Cr(VI) anions, present inside of the CCC coating, annihilate the adsorption of depassivating anions such as chloride ions [12]. The presence of trapped hexavalent chromium is responsible of the 'self-healing' ability of the coating under corrosion which remains a tremendous advantage driven by this species [9]. The determination and the control of the chemical form of hexavalent chromium in the coating are then the key to understand the properties of the chromate films and to find out some equivalent coatings. The mechanism is monitored over the whole pre-treatment and treatment steps. To describe the coating composition during its deposition and its chemical properties, both the etching solutions (pre-treatment) and the coatings (CCC treatment) were monitored by electrochemical and spectrometric techniques. The chemical composition and the microstructure features of the protective coated layers were next examined by scanning electron microscopy (SEM) and X-ray photoelectron spectroscopy (XPS).

The second part of this chapter aims to compare the performance of some potential CCC alternative coatings built up from different salts. The properties of these coatings are presented in **Table 1**.

http://dx.doi.org/10.5772/66604

Coating	Properties	References
Cr(III)	• Cracked coating • Small improvement of the corrosion resistance for bare alloy	[13]
Phosphate	• Longer stability under salt-spray conditions than zinc phosphate coatingall • Better corrosion resistance after painting than zinc phosphate coating	[14–16]
Zinc phosphate	• Thicker than magnesium phosphate coating • Fine zinc particles surrounded phosphate crystals and filled in the interstice of the insoluble phosphate • Microporous structure of the coating • Better adhesion of paint on the zinc phosphate coating than on chromate conversion coating • Very susceptible under salt-spray conditions • Better corrosion resistance than phosphate coating	[16–18]
PCC (permanganate conversion coating)	• Nearly crack-free coating • Average thickness of 230 nm after 90 s of immersion and increasing with continued immersion • Sufficient electrical conductivity • Poor crystallinity, comparable to chromate conversion coatings • Corrosion resistance inferior to chromate conversion coatings	[19, 20]
Permanganate/ phosphate	• Typical coating thickness, 4–6 μm • Equivalent or slightly better passive capability than the conventional Cr (VI)-based conversion treatment	[20–23]
Vanadium	• Self-healing ability similar to CCCs for magnesium alloys • Poor protection against corrosion	[24–28]
REEs (rare earth elements–based coating)	• Self-healing effect • Two-layer structure for cerium conversion coating • Adhesive weakness of the coating • Homogeneous and uniform conversion coating • Good adhesion to substrate with thickness of about 10 μm for lanthanum-based conversion coatings	[7, 28–30]

Table 1. Existing CCC (chromate conversion coating) alternative coatings.

On the basis of the identified chemical protection events, some existing and new alternative solutions have been classified in this study into two categories, A and B. This classification is done according to the chemical properties of the constitutive compounds of the treatment solutions used for the coating deposition. Ten own-made solutions and three industrial solutions commonly used for protection of light metal (Al-based) alloys have then been considered in order to test their efficiency on specific EV31A magnesium alloy. The corrosion protection properties in relation with the coating chemical composition were compared to CCC ones on the basis of stationary voltammetry and X-ray photoelectron spectroscopy collected data. They were evaluated in terms of their formation mechanism.

2. Chemical mechanism of chromate conversion coating

The well-known and currently used chemical process for magnesium protection consists in three different steps: degreasing, pickling and treatment. The process synoptic is detailed in **Figure 1**.

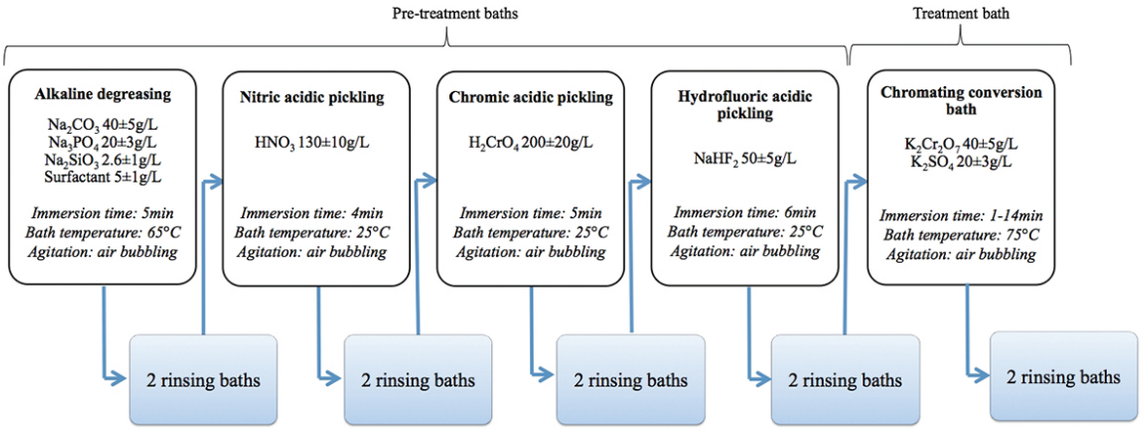

Figure 1. Etching process synoptic for the EV31A protection.

Each pre-treatment step participates in a chemical modification of the surface of the alloy (**Table 2**). These chemical compositions, determined by XPS after a rinsing step, are particularly important for the whole understanding of the deposit and the application of the future coating and on the protection properties against corrosion.

For bare EV31A, only carbon (C 1s), oxygen (O 1s) and magnesium (Mg 2p) signals were detected. The magnesium at the surface exits into two oxidation states: (0) and (+II), with Mg 2p components at 49.2 eV (Mg metal [31]) and around 50.5 eV corresponding to both $Mg(OH)_2$(s) and MgO(s) [32]. The examination of O 1s peak confirms the co-existence of the oxide and hydroxide forms with two corresponding components at 530.7 eV (MgO(s)) and 532.6 eV ($Mg(OH)_2$(s)). A small roughness (0.62 μm) is recorded in the tri-dimensional representation of the bare EV31A alloy and a very low corrosion potential (-1.61 $V_{/SCE}$) is measured which confirms the fact that EV31A alloy has to be protected against corrosion.

http://dx.doi.org/10.5772/66604

%At.		Bare EV31A	Alkaline degreasing	Nitric acid pickling	Chromic acid pickling	Hydrofluoric acid pickling
C		34.1	25.3	14.7	14.0	15.6
Cr	$Cr_2O_3(s)$	*	*	*	6.5	2.7
	$Cr(OH)_3(s)$	*	*	*	5.1	1.3
	$K_2CrO_4(s)$	*	*	*	4.7	0.4
F		*	*	*	*	14.0
Gd		*	*	0.1	*	0.1
Mg	$MgO(s)$	20.7	4.7	6.8	7.2	10.8
	$Mg(OH)_2(s)$					
	$MgF_2(s)$	*	*	*	*	7.1
	Mg (in PO_4 environment)	*	15.1	*	*	*
	Mg^0	9.9	0.7	21	*	1.1
N		*	*	2.4	*	*
Na		*	2.3		*	4.4
O		35.3	46.3	53.2	62.3	42.2
P		*	5.5	*	*	*
Zn		*	0.1	0.8	*	0.2
Zr		*	*	1	0.2	0.1

*Not present.

Table 2. XPS atomic composition (%At) of the coating during the pre-treatment process.

2.1. Cleaning of the surface

During the degreasing step, a redox reaction between the magnesium (0) of the EV31A alloy surface and water causes the apparition of Mg^{2+} (reaction (1))

$$2H_2O + Mg \rightleftarrows Mg^{2+} + H_2(g) + 2OH^- \quad (1)$$

XPS results clearly evidenced this trend as atomic percentage of Mg^0 (BE ~49.5 eV) drastically went down (~10% for bare alloy and 0.7% after degreasing). Under alkaline conditions (pH = 11), Mg^{2+} ions then react with the hydroxide ions OH^- to form $Mg(OH)_2(s)$.

Once withdrawn from the bath and before being rinsed, the surface of the alloy is kept in contact with the atmosphere and $Mg(OH)_2(s)$ dehydrates into magnesium oxide MgO(s).

Na_3PO_4 of the degreasing bath seems to interact directly with the alloy as Mg in a PO_4 environment was identified (BE ~51.4 eV). This detection should indicate the formation of $Mg_3(PO_4)_2(s)$, a compound responsible for the protection of the magnesium surface, in the case of phosphate coatings [14, 15]. But no significant improvement or diminution of the corrosion

resistance was observed: E_{corr} = -1.65 ± 0.04 V after the piece is dipped in the degreasing alkaline bath and the two rinsing baths, whereas E_{corr} = -1.61 ± 0.08 V for the bare alloy. It means that the layer of magnesium oxide /hydroxide formed at the surface would not act as a direct protective layer of the alloy against the corrosion. The observation of the microstructure confirms the absence of a surface modification (**Figure 2b**).

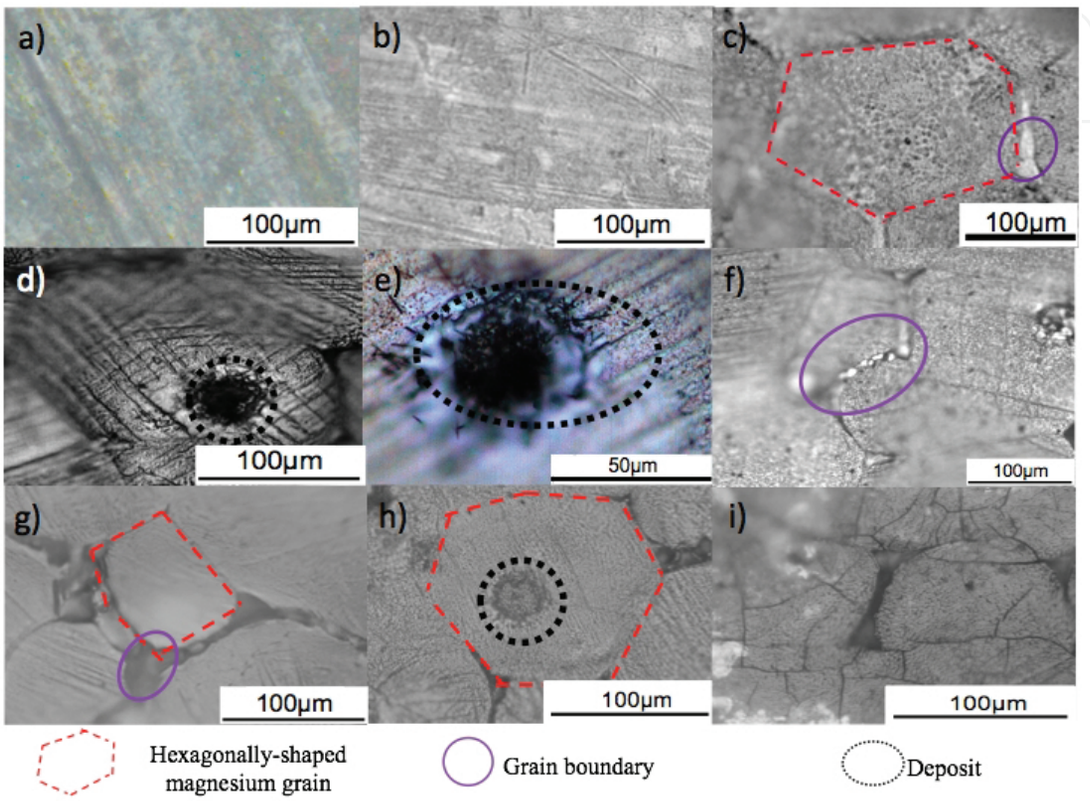

Figure 2. Surface of the EV31A alloy after being dipped in (a) bare alloy, (b) the alkaline-degreasing bath, (c) nitric acidic-pickling bath, (d)–(f) chromic acidic-pickling bath, (g) hydrofluoric acidic-pickling bath, (h) treatment bath (after 5 s) and (i) treatment bath (after 14 min).

The role of the alkaline degreasing bath is to remove the contamination on the surface of the alloy. The surfactant present in the bath is responsible for the removal of carbonated impurities which is confirmed by the XPS data (see **Table 2**, at.%C clearly decreases under degreasing process).

2.2. Increase of the surface roughness

With the nitric acidic-pickling bath, the magnesium in phosphate environment disappears (absence of Mg 2p component at 51.4 eV) and the oxide/hydroxide layer is highly damaged allowing the observation of the substrate (re-appearance of metal magnesium with Mg2p component at 49.2eV). In these acidic conditions, a main redox reaction occurs between the nitrate ions (E^0 = 0.96 V) and the magnesium (0) (E^0 = -2.36 V) at the surface of the alloy. This oxidative process dissolves Mg and some minor elements of EV31A are then detectable (e.g.,

http://dx.doi.org/10.5772/66604

Gd, Zn and Zr) (**Table 2**). Reaction (2), describing the oxidation of magnesium (0) by nitrate ions, leads to the solubilization of magnesium (II) in the bath and the formation of gaseous nitric oxide:

$$2NO_3^- + 8H_{aq}^+ + 3Mg \;\rightleftarrows\; 3Mg^{2+} + 4H_2O + 2NO(g) \tag{2}$$

The important difference of potential between these two species explains high reactivity in this bath and consequently the high surface roughness of the alloy surface (3.20 ± 0.40 μm instead of 0.62 ± 0.07 μm for the bare alloy) and the important weight loss of 130 g/m^2 measured after immersion in this bath.

Afterwards, with the immersion in the consecutive rinsing baths at neutral pH, the formation of $Mg(OH)_2(s)$ is renewed at the surface of the EV31A alloy.

Only a small improvement of the corrosion resistance is observed: ΔE_{corr} = +0.06 V in comparison with the bare alloy. The annual corrosion thickness increases to 227.3 μm/year and indicates a protection loss. This value could be correlated with the Mg^0 content, which went up to 21%. These data are in accordance with the previous conclusion discussing the minimized role of Mg oxide/hydroxide layer in the alloy protection.

Surface modification can be confirmed by **Figure 2c** with the appearance of hexagonally shaped grains of magnesium (red-dashed lines), the grain boundaries, rich in the previously cited minor elements (purple circle), appearing clearer than the grain.

The role of the nitric acidic-pickling bath is to dissolve the grains of magnesium, to make the grain boundaries denser by increasing the roughness; this would facilitate the deposition of a future layer. Indeed, when the two phases of the alloy are bare, a micro-current forms at the substrate surface due to a potential [33]. This difference of potential allows the preferential dissolution of one of the phases of the coating.

2.3. Activation of the surface in order to make it adhesive

In a solution, hexavalent chromium could exist as hydrochromate ($HCrO_4^-$), chromate (CrO_4^{2-}) and dichromate ($Cr_2O_7^{2-}$) ionic species. The proportion of each ion in the solution would depend on the pH and the concentration. During the chromic treatment step, the pH of the bath is 1.0 and the main species is $Cr_2O_7^{2-}$ [34]. This species reacts with magnesium (0) of the alloy (reaction (3))

$$Cr_2O_7^{2-} + 14H_{aq}^+ + 3Mg \;\rightleftarrows\; 2Cr^{3+} + 7H_2O + 3Mg^{2+} \tag{3}$$

The formed ions Cr^{3+} then react with H_2O (due to the acidic conditions) to form $Cr(OH)_3(s)$ which precipitates at the surface of the alloy due to its low K_s ($10^{-29.8}$) [35]. This precipitation begins at the centre of the magnesium grains (black-dotted circle) as seen in **Figure 2d** and **e** confirming the preferential reduction of chromium (VI) by magnesium.

The precipitation of $Cr(OH)_3(s)$ is minimal due to the low pH (below 2.0). For this reason, the chromium-based layer would not cover the entire surface of the alloy but it is thick enough to hide metal magnesium of the alloy (no XPS Mg (0) 2p component detected at 49.5 eV). This coating reduces the weight loss to 13 g/m^2 only and decreases the surface roughness (R_a): 1.80 ± 0.20 μm strongly, whereas it was 3.20 ± 0.40 μm after the nitric bath. Once rinsed twice, $Cr(OH)_3(s)$ dehydrates into $Cr_2O_3(s)$. An oxide/hydroxide magnesium layer is also formed in the same rinsing bath conditions. The atomic concentration in magnesium oxide/hydroxide is about 7.2%.

The role of the chromic-pickling bath is to deposit a first layer of chromic species ($Cr(OH)_3(s)$, $Cr_2O_3(s)$ and $K_2CrO_4(s)$) at the centre of the grains of magnesium. These species are responsible for the improvement of the corrosion resistance: $\Delta E_{corr} = +0.17\ V_{/SCE}$ in comparison with the bare alloy and the corrosion thickness decreases to 57.4 μm/year.

This first deposition acts as a nucleation layer that improves further the deposition of the protective coating.

Finally, in the last step of the pre-treatment process (hydrofluoric acidic-pickling bath), the sodium bifluorure $NaHF_2(s)$ is dissociated into sodium Na^+ and fluoride ions F^- (XPS BE Na 1s = 1071.7 eV [31]) and hydrofluoric acid HF. HF is classified as a weak acid (pKa = 3.20 [36]) and releases F^- and H^+ ions. The fluoride ions react with the dissolved magnesium (reaction (1)) to form $MgF_2(s)$ (B.E.= 50.9 eV) at the surface of the coating.

Due to weak value of their respective K_s ($10^{-11.15}$ for $Mg(OH)_2(s)$ and $10^{-8.15}$ for $MgF_2(s)$) [35], both compounds are formed on the surface of the alloy (7.1 %At for $MgF_2(s)$ in the Mg 2p spectrum beside 10.8 %At for $Mg(OH)_2(s)$ and MgO(s) components). The apparition of MgO(s) occurs later as explained previously.

The decrease of the corrosion potential of the immersed specimen in the hydrofluoric acidic-pickling bath ($E_{corr} = +1.54 \pm 0.06\ V_{/SCE}$) corresponds to the apparition of $MgF_2(s)$ into the coating and the diminution of $Cr(OH)_3(s)$, $Cr_2O_3(s)$ and $K_2CrO_4(s)$ contents (species responsible for the improvement of the corrosion resistance).

The detection in the XPS analysis of magnesium (0) and of minor elements (Gd, Zr and Zn) constitutive of the EV31A and the rise of the alloy surface roughness (2.30 ± 0.50 μm) indicate that the hydrofluoric-pickling bath has a similar role than the nitric acidic-pickling bath exposing the grain boundary (purple circle in **Figure 2g**). However, it is also responsible of a partial replacement of the layer of magnesium oxide/hydroxide with MgF_2 without a complete elimination of the chromic layer, which explains the very low weight loss (4.6 g/m^2). MgF_2 deposited on the surface is completely dissolved in the treatment bath, facilitating the deposition of the protective coating.

The different steps of the pre-treatment process assessed the preparation of the surface for the treatment step in order to make the coating adhesive on the alloy surface. They participated in cleaning the surface and making it rough and reactive for the coating deposition.

http://dx.doi.org/10.5772/66604

2.4. Coating deposition

The formation of the chromium coating needs several minutes to cover the entire magnesium surface. The coating begins to appear after an immersion time of 5 s at the centre of the hexagonally shaped magnesium grain, confirming the attack of dichromate on magnesium (**Figure 2h**). This first deposit is the result of a redox reaction that occurs very quickly (reaction (3)). This reaction induces a local pH raise at the alloy surface, favouring the precipitation of magnesium hydroxide and oxide with the deposition of chromium hydroxide and oxide. This coating expands to the grain boundaries as seen during the immersion in the chromic bath (**Figure 2i**)). The chemical composition of the coating is a function of the immersion time (**Table 3**).

%At.		2 min	6 min	8 min	12 min	14 min
Fe			0.4			
C		31.0	34.1	35.0	36.7	37.1
Cr	$Cr_2O_3(s)$	3.4	4.6	4.6	4.7	4.0
	$Cr(OH)_3(s)$	2.6	3.3	3.1	2.9	3.0
	$K_2CrO_4(s)$	1.1	1.7	2.2	1.1	1.4
F		7.8	0.3	0.1	0.4	0.4
K		0.2	0.6	0.4	0.1	0.4
Mg	$MgO(s)$	5.9	3.3	3.3	3.1	3.3
	$Mg(OH)_2(s)$					
	$MgF_2(s)$					
	Mg^0	3.2				
N		0.6	0.5	0.5	0.9	0.6
O		40.9	47.1	47.2	46.6	46.8
S		3.2	4.0	3.5	3.4	2.9
Zn		0.1	0.1	0.1	0.1	0.1

*Not present

Table 3. Atomic composition (%At) of the coating during the chromium conversion process on EV31A pieces after the pre-treatment step.

The quick growth of the chromium coating leads to the disappearance of magnesium (0) and the magnesium content tends to decrease from 17.9% (t = 0 min) to 5.9% after 2 min of immersion and is down to 3.3% after 6 min of immersion in the treatment bath (**Table 3**) and its replacement by chromium. Different chromium species exist ($Cr(OH)_3(s)$, $Cr_2O_3(s)$ and

CrO_3(s)/K_2CrO_4(s) (hard to differ with the XPS as all these environments get the same XPS Cr 2p BE)) and become predominant after 6 min of immersion in the bath. Peak assignments are made with respect to the reference compounds analysed in the same conditions, namely Cr_2O_3(s), $Cr(OH)_3$(s), CrO_3(s), K_2CrO_4(s) and $K_2Cr_2O_7$(s) [37, 38]. The concentrations of the chromium species increase during the first 6 min of immersion before stabilizing, indicating a complex surface chemical process and a homogeneous repartition into the coating.

Cr_2O_3(s) is issued from the dehydration of $Cr(OH)_3$(s) after the rinsing and drying steps. This dehydration gives the coating a surface morphology with plane domains separated with large cracked frontiers (**Figure 3**, zone 1).

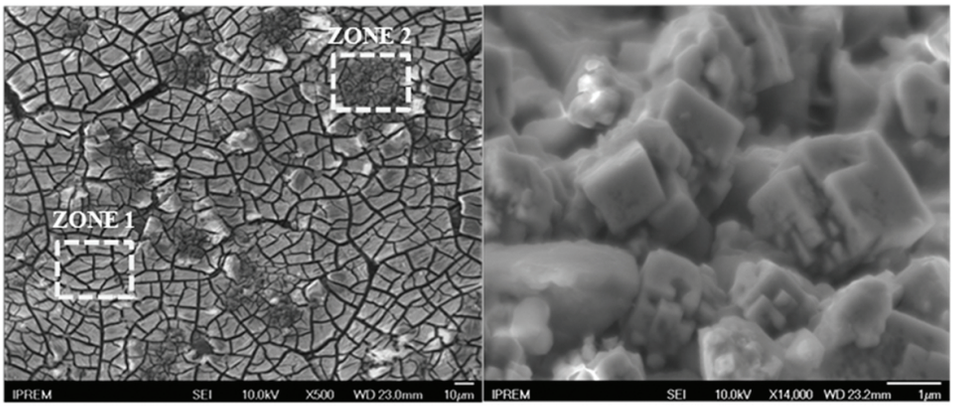

Figure 3. (a) High-resolution SEM image of large cracked frontiers (zone 1) and clusters (zone 2) on the surface after 6 min of treatment. (b) High-resolution SEM image of zoom in a cluster (zone 2).

The presence of K_2CrO_4(s) or CrO_3(s) in the coating is attributed to re-crystallization at the surface (**Figure 3**, zone 2). Actually, the Cr(VI) species trapped in the protective coating over alloys are generally known to be responsible for the 'self-healing' effect of the considered coating [12]. The presence of zinc in the coating remains minimal (around 0.1%).

At final, the deposition of the coating seems to occur during the first 6 min of immersion and induces the decrease of the surface roughness from 2.3 ± 0.5 μm before treatment to 1.4 ± 0.2 μm after 6 min of immersion. During the two first minutes of immersion, the coating spreads across the surface and covers it entirely. During the next 4 min, the layer thickens and keeps growing to reach 11 μm after 14 min of immersion in the bath.

The corrosion resistance is improved to +0.2 V after 2 min of immersion in the chromium bath. The final corrosion resistance presents a ΔE_{corr} = +0.3 V after 6 min of immersion and stabilizes around this value with increasing immersion times. This corrosion potential and the annual corrosion thickness stay low (E_{corr} = -1.4 ± 0.1 $V_{/SCE}$, e = 50 ± 10 μm/year) and the application of a painting should be necessary to obtain a total protection against corrosion. Another way could be the replacement of chromium by an alternative coating.

http://dx.doi.org/10.5772/66604

3. Alternative conversion coatings

New alternative conversion coatings have been proposed since few years to replace CCCs due to the recent limitations and the future interdiction of the use of chromium (VI) (**Figure 4**). These coatings present proper action modes and their own mechanisms and properties for the protection of Mg.

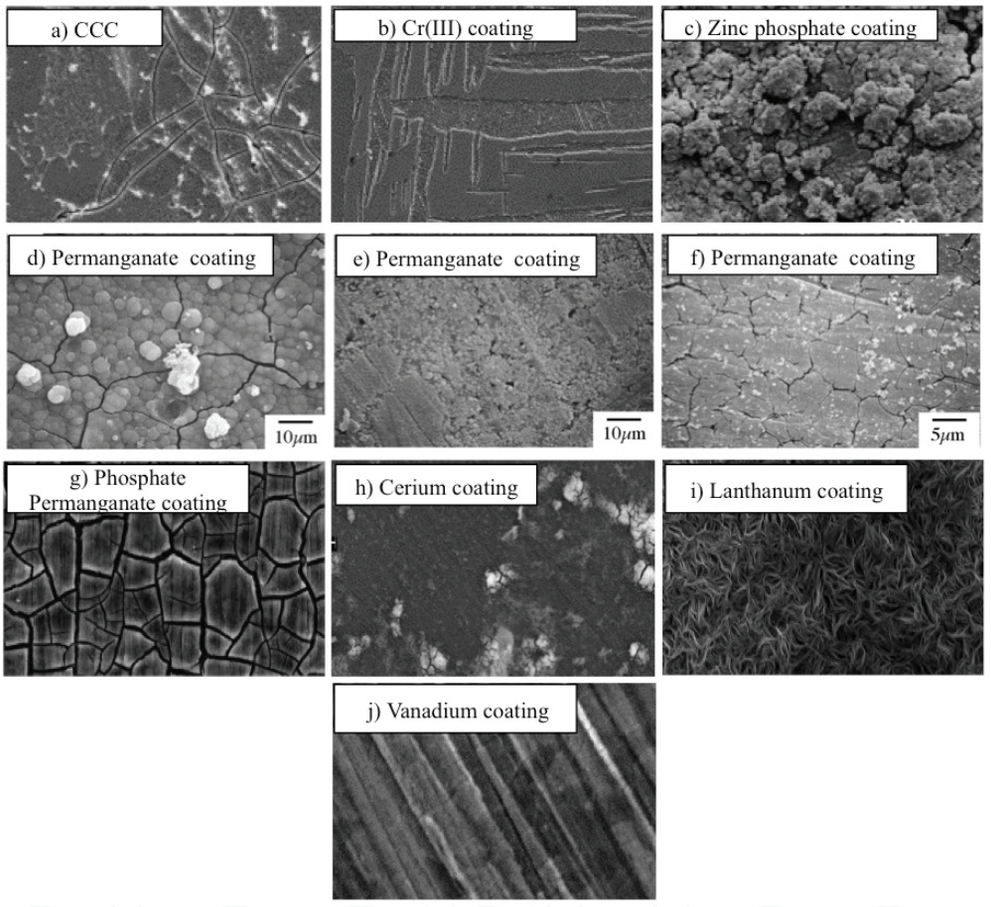

Figure 4. SEM (scanning electron microscopy) images of coatings obtained with treatment baths containing (a) Cr (VI) [12], (b) Cr (III) [12], (c) zinc phosphate [10], (d) permanganate with HNO_3 [19], (e) permanganate with HF [19], (f) permanganate with HCl [19], (g) phosphate permanganate [23], (h) cerium [39], (i) lanthanum [30] and (j) vanadium [24].

3.1. Cr(III)-based coatings

Cr(III)-based coatings involve a redox reaction: the metal is oxidized by an oxidant added to the bath. This oxidant (H_2O, NO_3^-, etc.) is simultaneously reduced as shown in reactions (1) and (4) [40, 41]

$$Mg + NO_3^- + 2H^+_{aq} \leftrightarrows Mg^{2+} + NO_2^- + H_2O \quad (4)$$

A local pH increase is caused by the hydronium ion consumption (reaction 4) or the OH^- formation (reaction 1). This pH variation causes the precipitation of trivalent chromium as an insoluble hydroxide and then oxide.

An example of Cr(III) treatment gives a 90-nm coating made of 60% $Cr(OH)_3$(s) and 40% Cr_2O_3(s) (**Figure 4b**) [12]. The film presents a smooth and continuous structure with no cracks [13]. Generally, the corrosion resistance is less effective with Cr(III) coatings than with CCCs [6, 12]. This can be attributed to the difference in thickness of the two films and to the presence of mobile Cr(VI) species in CCCs that allow the repassivation of flaws and corrosion pits [6, 12].

Actual commercial Cr(III) solutions are made with CrF_3 and $(NH_4)_2ZrF_6$. These solutions present a better protection against corrosion: $\Delta E_{corr} = +0.60 \pm 0.1$ V. The annual corrosion depth is about 11 ± 1 μm/year, whereas it is 50 ± 10 μm/year for chromium VI coatings.

Cr content is lower than Cr(VI) solution: 6–7 At% for commercial Cr(III) solution and 9–10 At % for chromium VI bath. The main difference in the coating composition remains in the fluoride content: 13–14 At% for commercial Cr(III) solution and 0.1–0.2 At% for chromium VI bath. Could fluoride compounds with chromium or magnesium increase the protection against corrosion? An MgF_2 layer does not have this property as seen in the previous section, but a mix of chromium and magnesium fluorides could increase this protection in comparison to chromium and magnesium oxides and hydroxides.

3.2. Phosphate-based conversion coatings

Phosphate coatings are more environmentally friendly than CCCs, and many scientists have tested films deposited from phosphate solutions. Currently, this process is one of the most studied alternatives to CCCs on magnesium alloys. Phosphate coating on zinc, steel and aluminium is already a well-known process [42].

In contrast to Cr(VI), phosphate cannot oxidize the surface of an alloy. Phosphate can only passivate alloy surfaces. Without the presence of an oxidant, the oxidation of magnesium only occurs due to the reduction of water according to reaction (1).

To create an efficient film, it is necessary to add an oxidant to the bath to increase the rate of magnesium alloy oxidation [43]. The main oxidants used are NO_3^- or H_2O_2 [43]. Nitrites can be added with nitrates to further accelerate oxidation.

In the phosphate bath, an equilibrium exists among all forms of the orthophosphoric acid that can dissociate by successively liberating protons. The dominant form of orthophosphoric acid depends on the solution pH. Phosphate baths are mainly around pH 3.0 [14, 17, 18]. In these baths, H_3PO_4 and $H_2PO_4^-$ are the primary species according to their pKa values: $pKa_1 = 2.15$, $pKa_2 = 7.20$ and $pKa_3 = 12.35$ [35].

Reactions (1) and (4) lead to a local pH increase at the alloy surface and, consequently, to the modification of the phosphate species to HPO_4^{2-} and PO_4^{3-}. The phosphate ions PO_4^{3-} react with Mg^{2+} to form $Mg_3(PO_4)_2$(s) ($K_s = 10^{-25.2}$ [35]) as shown in reaction (5) [14]

http://dx.doi.org/10.5772/66604

$$3Mg^{2+} + 2PO_4^{3-} \leftrightarrows Mg_3(PO_4)_2(s) \quad (5)$$

Another possibility for the formation of $Mg_3PO_4(s)$ has been considered [42]. The chemical reactions between the oxidized base metal Mg and the phosphate can be described by reactions (6)–(8):

$$Mg + 2H_2PO_4^- + 2H^+_{aq} \leftrightarrows Mg(H_2PO_4)_2(s) + H_2(g) \quad (6)$$

$$Mg(H_2PO_4)_2(s) \leftrightarrows MgHPO_4(s) + H_3PO_4 \quad (7)$$

$$3MgHPO_4(s) \leftrightarrows Mg_3(PO_4)_2(s) + H_3PO_4 \quad (8)$$

The value of the thermodynamic function H^0 for $Mg_3PO_4(s)$ and $Mg(OH)_2(s)$ is 3780.6 and 924.2 kJ/mol, respectively. Consequently, Mg^{2+} preferentially bonds with PO_4^{3-}, which explains the absence of $Mg(OH)_2(s)$ in the coating [14]. $Mg_3PO_4(s)$ is so the main compound of the coating and responsible for the corrosion protection in these kinds of coatings. Its density (2.74 g/cm^3) is two times lower than the Cr_2O_3 (5.22 g/cm^3) [36]. This property could be a hypothesis to explain the lower corrosion resistance of these coatings in comparison to CCCs (**Table 4**).

In the case of Mg-Li alloys, the deposition occurs mainly on the β-phase where the redox reactions (1) and (4) occur. A conversion film forms as shown in reactions (5)–(8) [14, 15]. The film grows until an equilibrium is established between film dissolution and formation [15].

If other divalent cations, such as Ca^{2+}, are added to the bath and hydroxide ions are present at the alloy surface, then HPO_4^{2-} and PO_4^{3-} preferentially bond to form insoluble $CaHPO_4{,}2H_2O(s)$ [14, 44].

To strengthen the corrosion resistance of the coating, Zn(II) salts are added to create an insoluble layer of $Zn_3(PO_4)_2(s)$. Sometimes, ZnO is added to the bath because the addition of a metallic oxide can influence the microstructure of a phosphate coating and make the coating denser and thinner [18]. Generally, the compositions of all the zinc phosphate baths are similar: a buffer made with orthophosphoric acid H_3PO_4, dihydrogen phosphate $H_2PO_4^-$ and NO_3^- with NO_2^- as an accelerating agent. The differences stay in the nature and the concentration of the zinc salt.

The deposition mechanism of zinc phosphate coatings begins with the phosphate precipitation on anodic areas [42, 47]. In these areas, metal alloy is oxidized while water is reduced from the surface, leading to the increase of pH [42]. The local increase of pH allows the precipitation of $Mg_3(PO_4)_2(s)$ ($K_s = 10^{-25.2}$ [35]) and more especially of insoluble $Zn_3(PO_4)_2{,}4H_2O(s)$ ($K_s = 10^{-35.3}$ [35]) as shown in Eq. (9) [42]

Alloy	Bath characteristics			Coating characteristics			Ref
	Compounds	Concentration	pH	Composition	j_{corr} (μA/cm²)	E_{corr} ($V_{/SCE}$)	
Mg-8.8Li	$NH_4H_2PO_4$	25 g/L	3	$CaHPO_4.2H_2O$(s)	0.2	-1.58	[14]
	$Ca(NO_3)_2$	25 g/L		$Ca_3(PO_4)_2$(s) $Mg_3(PO_4)_2$(s)			
AM60	H_3PO_4	7.4 mL	3	*n.d*	10,000	-0.90	[42]
	Na_2HPO_4	20 g/L					
	$NaNO_3$	3 g/L					
	$NaNO_2$	1.84 g/L					
	$Zn(NO_3)_2$	1.84 g/L					
	NaF	1 g/L					
AZ91D	H_3PO_4	17.5 g/L	3	$Zn_3(PO_4)_2{\cdot}_4H_2O$(s)			[17]
	ZnO	3.2 g/L		Zn $AlPO_4$(s)			
	NaF	1.7 g/L		$MgZn_2(PO_4)_2$(s)			
	$NaNO_3$	0.17 g/L		$Mg_3(PO_4)_2$(s)			
	$NaNO_2$	0.83 g/L					
	$C_4H_4O_6$	2.2 g/L					
	Amine	0.18 g/L					
AZ91D	H_3PO_4	0.065 mol/L	2.4	$Zn_3(PO_4)_2.4H_2O$(s)	*n.d*	-1.17	[18]
	ZnO	0.0029 mol/L		Zn(s)			
	$Zn(NO_3)_2$	0.102 mol/L					
	NaF	0.040 mol/L					
	$NaClO_3$	0.0028 mol/L					
	NH_3	0.0034 mol/L					
	Amine	0.007 mol/L					
AZ31	H_3PO_4	7.4 mL/L	3	$Zn_3(PO_4)_2.xH_2O$(s)	*n.d*	-1.37	[45]
	$NH_4H_2PO_4$	20 g/L					
	$NaNO_3$	1.84 g/L					
	$NaNO_2$	3 g/L					
	$Zn(NO_3)_2$	5 g/L					
	NaF	1 g/L					
AZ31	H_3PO_4	0.10 mol/L	3.07	$Zn_3(PO_4)_2{\cdot}4H_2O$(s)	0.54×10^{-5}	*n.d*	[46]
	$NH_4H_2PO_4$	0.034 mol/L		$MgHPO_4{\cdot}3H_2O$(s)			
	$NaNO_3$	0.021 mol/L		$Mg_3(PO_4)_2$(s)			
	$NaNO_2$	0.042 mol/L		$AlPO_4$(s)			
	$Zn(NO_3)_2$	0.068 mol/L		Al_2O_3(s)			
	NaF	0.024 mol/L		$Al(OH)_3$(s)			
				MgO(s) and/or $Mg(OH)_2$ (s)			

Table 4. Composition of phosphate baths and their respective coating compositions and properties.

http://dx.doi.org/10.5772/66604

$$3Zn^{2+} + 3Mg + 4H_2PO_4^- + 4H_2O \leftrightarrows Zn_3(PO_4)_2(s),4H_2O(s) + Mg_3(PO_4)_2(s) + 2H^+_{aq} + 3H_2(g) \quad (9)$$

More precisely, the resulting amorphous layer consists of mixed phosphates of zinc and alloy magnesium (reaction 10). This first layer is the base for the development of crystal nuclei of zinc phosphate $Zn_3(PO_4)_2,4H_2O(s)$. This theory is based on the existence of $ZnPO_4^-$ resulting from the formation (reaction (11)) and then the dissociation (reaction (12)) of $Zn(H_2PO_4)_2,2H_2O$ in the bath [17]

$$Mg + 2H^+_{aq} + 2ZnPO_4^- \leftrightarrows MgZn_2(PO_4)_2(s) + H_2(g) \quad (10)$$

$$Zn^{2+} + 2H_2PO_4^- + H_2O \leftrightarrows Zn(H_2PO_4)_2,2H_2O \quad (11)$$

$$Zn(H_2PO_4)_2,2H_2O \leftrightarrows ZnPO_4^- + H_2PO_4^- + 2H^+_{aq} + 2H_2O \quad (12)$$

The coating (**Figure 4c**) has a double-layer structure, an inner amorphous layer and a crystal outer layer. The inner layer consists of an amorphous dense inner layer made of $MgZn_2(PO_4)_2(s)$, $Mg(OH)_2(s)$ and/or $MgO(s)$ and some small amounts of $AlPO_4(s)$, $Al_2O_3(s)$ and/or $Al(OH)_3(s)$. The outer porous crystal layer is composed of crystal hopeite, $Zn_3(PO_4)_2(s)$ [46]. This layer is generally porous due to the presence of cracks and flaws [48].

The detection of aluminium in the coating comes from its incorporation in several alloys. Its presence in the coating slows down the formation of the phosphate films on magnesium surfaces. Fluoride ions can be added to release Al complexes AlF_6^{3-} from the cathodic sites. This complexion influences the zinc phosphate film formation by increasing the number of nuclei and allowing the formation of a more compact layer [42]. Sodium fluoride NaF precipitates aluminium ions in the solution to form $Na_3AlF_6(s)$ [42].

Zinc phosphate improves the corrosion resistance relative to a simple phosphate coating [17, 18, 42, 45, 47]. Higher corrosion potentials are obtained with zinc phosphate baths (**Table 4**). The density of this compound is 3.998 g/cm^3 [36]. The presence of this compound in the coating of magnesium phosphate increases the density of the layer and could be responsible for better corrosion resistance.

The protection provided by phosphate alone is not equivalent to a CCC due to the formation of a low dense layer of $Mg_3(PO_4)_3$. On the other hand, the zinc phosphate coating seems to provide better corrosion resistance than the CCC. Indeed, the corrosion potential is from -1.37 to -0.9 $V_{/SCE}$ for this coating, and it is of -1.4 ± 0.1 $V_{/SCE}$ for the Cr(VI) coating.

3.3. Permanganate-based conversion coatings

The coatings based on permanganate solutions are named PCCs (permanganate conversion coatings). These solutions contain Mn(VII) species acting as oxidant agents on the alloy. The reduced Mn(IV) species coat and passivate the substrate as shown in Eqs. (13) and (14) [49].

$$2MnO_4^- + 3Mg + 8H_{aq}^+ \leftrightarrows 2MnO_2(s) + 3Mg^{2+} + 4H_2O \quad (13)$$

$$2MnO_4^- + 4Mg + 10H_{aq}^+ \leftrightarrows Mn_2O_3(s) + 4Mg^{2+} + 5H_2O \quad (14)$$

The protective species are MnO_2 or Mn_2O_3 and have similar or superior densities (respectively 5.0 and 9.6 g/cm^3) than Cr_2O_3 formed in the case of CCC [36]. The corrosion protection properties are close but not better than CCC (E_{corr} = -1.5 ± 0.1 $V_{/SCE}$ in comparison to E_{corr} = -1.4 ± 0.1 $V_{/SCE}$ for Cr(VI) coating). The annual corrosion depth is worse in the case of PCC (e = 100 ± 10 μm/year in comparison to e = 50 ± 10 μm/year for Cr(VI) coating).

PCC baths still possess the advantage of not requiring the need to be heated [49]. Moreover, PCC process does not form protective inorganic polymer coatings like CCC, which makes it less affected by heat than CCCs and are more convenient for painting [49].

Table 5 groups the PCC baths that are usually tested on magnesium alloys. These baths contain $KMnO_4$ associated with different strong acids [19, 49]. The nature and the concentration of the acid affect the structure and the composition of the coating [19]. **Figure 4d–f** shows the different morphologies of PCCs. The addition of HNO_3 affects the surface of the coating, forming clusters of particles (**Figure 4d**) [19]. With the addition of HF (**Figure 4e**), the coating has an amorphous structure. This film is thinner than the coating deposited in a bath containing HNO_3, and the deposition rate is slower [19]. The thinner film can be explained by the reaction of fluorine ions with magnesium to produce insoluble magnesium fluoride $MgF_2(s)$, creating a passivating layer that prevents any further dissolution of magnesium [19]. Coatings dipped in the HF and the $KMnO_4$ solutions are composed mainly of $MgF_2(s)$ and manganese oxides ($MnO_2(s)$, $Mn_2O_3(s)$ and $Mn_3O_4(s)$), while the coatings formed in the $HNO_3/KMnO_4$ bath contain Mg and Mn oxi-hydroxides. More cracks in the coating can be observed when HCl is present in the solution (**Figure 4f**). The role of an addition of an acid to a permanganate bath on the protective properties of the final coating has not been quantified but the coatings characteristics (thinner film with HF, cracks with HCl and presence of clusters with HNO_3) may decrease the corrosion resistance of the coating.

Permanganate coatings provide an alternative to CCC but they do not provide good corrosion resistance. Another problem that prevents PCCs from replacing CCCs is the stability of the bath pH. Important pH variations occur when PCC baths are used and the alloys are dipped in the solution. The attack of MnO_4^- on Mg alloy surfaces consumes H^+_{aq} ions (reactions 13 and 14), increasing the pH of the solution. The addition of $Na_2B_4O_7$ to an HCl bath has a buffering effect and stabilize the pH of the bath [19, 49]. However, the Registration, Evaluation, Authorization and Restriction of Chemicals added tetraborate products to the list of substances of very high concern (SVHC), and their use is now limited and will be completely forbidden in a few years. Other compounds must be found to stabilize the pH of PCC baths.

http://dx.doi.org/10.5772/66604

Alloy	Bath characteristics		Coating characteristics	Ref
	Compounds	Concentration mol/L	Composition	
AZ91D	$KMnO_4$	0.02	MnO_2(s) Mn_2O_3(s)	[19]
	HNO_3	0.02–0.2	Mn_3O_4(s)	
			Mg oxide/hydroxide	
AZ91D	$KMnO_4$	0.02	Mn oxide/hydroxide	[19]
	HCl	0.02–0.2	B oxide/hydroxide Mg oxide/hydroxide	
	$Na_2B_4O_7$	unknown		
AZ91D	$KMnO_4$	0.02	MnO_2(s) Mn_2O_3(s)	[19]
	HF	0.02–0.2	Mn_3O_4(s) MgF_2(s)	
			Mg oxide/hydroxide	

Table 5. Composition of permanganate baths and their respective coating compositions and properties.

3.4. Permanganate/phosphate-based conversion coatings

The combination of phosphate and permanganate has been considered as a solution to avoid the pH increase in baths. In a potassium permanganate bath, monopotassium dihydrogenophosphate (KH_2PO_4) or manganese hydrogenophosphate ($MnHPO_4$) is added as a buffer [3]. The reactions of the deposit are the same as discussed previously: the oxidation of magnesium and the reduction of Mn(VII) consume the H^+_{aq} responsible for the pH increase, allowing the phosphate species to precipitate at the metal surface (reactions (5), (13) and (14)) [23, 50].

The grain boundaries act as cathodes, and grains function as anodes, forming local cell effects. Meanwhile, hydrogen and phosphate ions are consumed at the substrate/solution interface, causing a pH increase. This phenomenon favours the formation of $Mg_3(PO_4)_2$(s) deposits (**Figure 4g**).

$Mg(OH)_2$(s), MgO(s), MnO_2(s) and Mn_2O_3(s) can be found in the coatings as detailed on reactions (15) and (16) (**Table 6**). The presence of Al in the alloys leads to the formation of $Al(OH)_3$(s), Al_2O_3(s) and $MgAl_2O_4$(s) as shown in reactions (17) (**Table 6**) [22]

$$2MnO_4^- + 5Mg + 12H_{aq}^+ \leftrightarrows 2MnO(s) + 5Mg^{2+} + 6H_2O \quad (15)$$

$$2MnO_4^- + 4Mg + 10H_{aq}^+ \leftrightarrows Mn_2O_3(s) + 4Mg^{2+} + 5H_2O \quad (16)$$

$$MgO(s) + Al_2O_3(s) \leftrightarrows MgAl_2O_4(s) \quad (17)$$

MnO_4^- species is also detected in the coating (**Table 6**). It has been trapped during the formation of the coating. Its presence could be responsible for a 'self-healing' effect as in the case of chromium VI coatings. MnO_4^- ions have not been detected in the 'permanganate-only' coatings.

	Bath characteristics				Coating characteristics					
Alloy	**Compounds**	**Concentration (g/L)**	**Immersion time (s)**	**pH**	**Composition**	j_{corr} **(μA/cm²)**	E_{corr} **(V_{SCE})**	***e*** **(mm/year)**	**Thickness (μm)**	**Ref**
Mg alloy (10%Li 1%Zn)	**$KMnO_4$** **KH_2PO_4**	40 50	1200	*n.d*	$Mg(OH)_2$(s) MgO(s) Mn_2O_3(s) MnO_2(s) K and P detected	*n.d*	-1.57	*n.d*	*n.d*	[33]
AZ91D	**$KMnO_4$** **KH_2PO_4** **H_3PO_4**	40 150 *n.d*	600	3–6	MgO(s) $Mg(OH)_2$(s) MnO_2(s) Mn_2O_3(s) $KMnO_4$	585.8	–1.40	13.2033	7–10	[5]
EV31A	**$KMnO_4$** **$MnHPO_4$**	40 75	300	3.5	MgO(s) $Mg(OH)_2$(s) MnO_2(s) Mn_2O_3(s) $KMnO_4$	0.3	–0.38	7.0×10^{-3}	*n.d*	
EV31A	**$KMnO_4$** **$MnHPO_4$**	40 150	300	3.5	MgO(s) $Mg(OH)_2$(s) MnO_2(s) Mn_2O_3(s) $KMnO_4$	0.06	-0.24	1.3×10^{-3}	*n.d*	
AZ91D	**$KMnO_4$** **$MnHPO_4$**	20 60	600	*n.d*	MgO(s) $Mg(OH)_2$(s) MnO_2(s) Mn_2O_3(s) $MgAl_2O_4$(s) Al_2O_3(s) $Al(OH)_3$(s)	18	-1.50	*n.d*	*n.d*	[22]
AZ91D	**$MnHPO_4.2H_2O$**	*n.d*	1800	*n.d*	Mn, O, P, Mg, Al	*n.d*	*n.d*	*n.d*	10	[3]
AM60B	**$NH_4H_2PO_4$** **$KMnO_4$** **H_3PO_4**	100 20 *n.d*	1200	3.5	*n.d*	*n.d*	*n.d*	*n.d*	*n.d*	[21]

Table 6. Composition of permanganate/phosphate baths and their respective coating compositions and properties.

The coating thicknesses are between 7 and 10 μm [5]. The conversion coating thickness decreased gradually with the increase of the pH value and the concentration of KH_2PO_4 in the bath. Below pH 3, a non-compact surface layer is formed because manganese is under the soluble Mn^{2+} form and not the protective MnO_2. Around pH 5, the formation of the coating is too slow due to the quick main precipitation of $Mg_3(PO_4)_2$ [5, 51]. The conditions are optimum when the concentration of KH_2PO_4 is maximum (150 g/L) and the pH fixed between 3.5 and 4.0 to form a coating made essentially with MnO_2 and $Mg_3(PO_4)_2$.

The good corrosion resistance of the permanganate-phosphate coatings allows considering this solution as a serious alternative to chromium coatings. Indeed, the immersion for 10 h in conventional corrosive electrolyte-artificial seawater (3.5 wt.% NaCl solution) does not present any trace of corrosion whereas only 300 s of immersion of the bare alloy in the same solution

http://dx.doi.org/10.5772/66604

is sufficient to observe corrosion pits on the surface of the alloy [33]. Chromium VI coating presents several corrosion pits after less than 4 h in the same conditions.

The corrosion protection properties are clearly better than CCC (E_{corr} = -0.3 ± 0.1 $V_{/SCE}$ in comparison to E_{corr} = -1.4 ± 0.1 $V_{/SCE}$ for Cr(VI) coating) (**Table 6**). The annual corrosion is also better in the case of permanganate/phosphate coatings (e = 1–7 ± 10 μm/year in comparison to e = 50 ± 10 μm/year for Cr(VI) coating).

The presence of aluminium in the final coating (when this element participates in the composition of the Mg alloys studied) does not disturb its corrosion resistance properties.

These results clearly indicate that permanganate/phosphate coatings present better corrosion resistance properties than CCCs for the protection of magnesium alloys due to the dense MnO_2/Mn_2O_3 layer mixed with $Mg_3(PO_4)_2$(s)

3.5. Vanadium-based coatings

Self-healing properties similar to the CCCs can also be obtained by adding vanadium-based oxyanions to the coating. Vanadium solutions are generally used as corrosion inhibitors in many paints or pigments [27].

The coatings obtained with a vanadium solution of 50 g/L are uniform and compact (**Figure 4j**). Their thickness is about 2.0 ± 0.5 μm [27]. The vanadium oxides that composed these coatings are mostly unidentified.

Vanadium coatings present good corrosion protection properties. Indeed, the vanadium coatings immersed in a 3.5% NaCl solution present, respectively, 15, 7 and 2 pits/cm^2 for the samples treated in 10, 30 and 50 g/L solution, whereas 50 pits/cm^2 can be observed on the surface of the polished alloy [26]. The size of the pits decreases also on vanadium coatings. The vanadium species responsible for the corrosion resistance are vanadium oxides [40].

The optimal conditions are obtained with a 50 g/L vanadium solution and pH 7. An increase of the pH from 7 to 9 had a negative effect on the corrosion protection performance of the coating [27]. The vanadium layer loosely adhered to the substrate alloy and the surface was severely corroded and covered with pits.

The increased corrosion resistance of the coated samples at 50 g/L and pH 7 is explained by the self-healing action that blocked the pitted areas from corrosive attack and other surface defects [27]. It seems that the formation of a vanadium oxide layer plays a distinct role in healing cracks in coating surfaces and repairing pits, and hence improving the overall localized corrosion resistance. Coatings formed in a 50 g/L vanadium solution are more effective than the other treatments with lower vanadium concentrations in reducing the number of pits due to the self-healing ability of the films and the 'buffer effect' of the vanadium-rich oxide layers that reject the corrosive chloride ions from the surface of the magnesium substrate [27].

Vanadium coating seems to be one serious option for the replacement of CCC. The self-healing ability of vanadium coatings due to their rich oxide layer is an important advantage. However, vanadium coatings have been responsible for worsening the corrosion of the magnesium alloy

EV31A [52]. This unexpected behaviour has been explained by the formation of multi-oxide layers of vanadium in addition to the alloying elements Zr, Nd and Zn at the surface, resulting in heterogeneous coatings [52]. The effectiveness of the coating directly depends on the composition of the alloy. This phenomenon has been only observed for vanadium coatings and not for the other alternatives to CCCs

3.6. Rare earth elements–based coatings

Among the 17 REEs, cerium and lanthanum are the most commonly used for conversion coating. The corrosion resistance of magnesium is improved by adding a small amount of REEs, although an excessive addition of REEs detract from the corrosion resistance. The optimum REEs content is between approximately 0.3 and 0.5wt% of the alloy [29].

When the alloy is dipped in one of the conversion solutions (listed in **Table 7**), the preformed hydroxide film on the substrate surface immediately dissolves. After that, the primary anodic dissolution reaction of magnesium occurs simultaneously with the reduction of hydronium ions [53]. The addition of oxidants, such as NO_3^- or H_2O_2, can favour oxidation [40, 54]. At the same time, the formation of OH^- increases the pH at the interface between the substrate and the solution.

Alloy	Bath characteristics				Coating characteristics			
	Compounds	Concentration	Immersion time (s)	pH	Composition	j_{corr} (μA/cm²)	E_{corr} (V_{SCE})	Ref
Mg-8.5Li	**$Ce(NO_3)_3$** **$La(NO_3)_3$** **$KMnO_4$**	2 g/L 2 g/L 2 g/L	300	4.0	La_2O_3(s) CeO_2(s) Mn_2O_3(s) MnO_2(s)	*n.d*	-1.5	[53]
Mg-8Li	**$La(NO_3)_3$**	5 g/L	1200	5.0	$La(OH)_3$(s)		-1.3	[30]
AZ63	**$CeCl_3$** **H_2O_2**	10 mg/L 50 mL/L	6 × 30	*n.d*	*n.d*	1.05×10^3	-1.49	[39]
AZ31	**$Ce(NO_3)_3$**	0.05 mol/L	*n.d*	3.6	CeO_2(s)	*n.d*	*n.d*	[29]
WE43	**$Ce(NO_3)_3$**	0.05 mol/L	300	3.6	*n.d*	*n.d*	*n.d*	[56]
WE43	**$La(NO_3)_3$**	0.05 mol/L	300	3.6	*n.d*	*n.d*	*n.d*	[56]
WE43	**$Pr(NO_3)_3$**	0.05 mol/L	300	3.6	*n.d*	*n.d*	*n.d*	[56]
AZ31	**$Ce(NO_3)_3$** **H_2O_2**	10 g/L 20 mL/L	300	*n.d*	CeO_2(s) CeO(s) Ce_2O_3(s) MgO(s) $Mg(OH)_2$(s) Al^2(s)	*n.d*	*n.d*	[40]

Table 7. Composition of REEs (rare earth elements–based coating) baths and their respective coating compositions and properties.

For cerium baths, if the interfacial pH value is high enough, then Ce^{3+} precipitates on cathodic sites to form $Ce(OH)_3$(s) [40, 54]. Coating formation is fast, and it is mainly controlled by the production of OH^- at the surface of the alloy. As coating formation proceeds, the surface is covered gradually with cerium hydroxide and then oxide. The rate of coating formation

http://dx.doi.org/10.5772/66604

gradually slows down. A dense Ce-based conversion coating is obtained on the surface of magnesium alloys. The conversion coating consists of a mixture of trivalent and tetravalent cerium oxides. Exposure to the atmosphere causes the oxidation of $Ce(OH)_3(s)$ to $Ce(OH)_4(s)$ and the dehydration of the hydroxides to oxides. Consequently, the Ce(IV) content is higher at the coating surface than at the inside of the coating [29]. The conversion coating (**Figure 4h**) consists of a mixture of $CeO_2(s)$ and $Ce_2O_3(s)$ [30, 53]. The inside and surface layers have different morphologies. It has been calculated that approximately 61% of the cerium species in the coating surface and 45% of the cerium species in the inside area exist in a tetravalent state [29].

When lanthanum (La) solutions are used, they contain $La(NO_3)_3$ in the range of 2–16.3 g/L [30, 55, 56]. The deposition mechanisms of these coatings are similar to those of the cerium coatings. The conversion films (**Figure 4i**) consist of mixtures of $La(OH)_3(s)$, $La_2O_3(s)$, $Mg(OH)_2(s)$, MgO(s) and $Al_2O_3(s)$ [30, 53]. Despite numerous studies on Ce coatings, the greatest corrosion resistance was obtained with La, although the reproducibility of those results was poor [55].

One of the important effects of the REEs on corrosion resistance is the 'scavenger effect'. Indeed, REEs create intermetallic compounds with impurities, cancelling the influence of some minor elements, such as Cl and Fe, on the corrosion resistance [55]. Indeed, the corrosion potential of these coatings varies between -1.50 and -1.30 V as shown in **Table 7**, which is comparable to the values found for CCCs (between -1.30 and -1.50 V) [29]. To improve the corrosion resistance, the presence of the same REE in the alloy and in the conversion bath is advised [55]. The corrosion resistance of the coated alloy is improved if the REEs content in the alloy equals 0.3 wt% Ce or is less than 0.1 wt% La [55]. REE coatings are the only baths that provide this 'scavenger effect' with properties as interesting as the self-healing ability of CCCs. However, an adhesive weakness of a cerium conversion coating on AZ31 alloy was noted where the surface layer was easily peeled off with an adhesive tape [29]. The adhesion between the surface layer and the inside layer of the coating was much weaker than between the inside layer and the metallic substrate.

4. Conclusion

The actual process for the protection of magnesium alloys against corrosion uses chromium VI baths. This process needs an initial four-step pre-treatment to obtain a high-performance coating. This step is essential for preparing the surface to promote the anchorage of the protective coating in the treatment bath. Then, the nitric acidic bath is responsible for a strong attack of the alloy surface to increase the roughness of the surface in order to improve adhesion. The chromic acid–pickling bath initiates the chromate coating deposition (thin layer) at the centre of the magnesium grains. The hydrofluoric acid–pickling bath allows the deposition of an MgF_2 layer, making the surface more reactive for further coating deposition. The first deposition of chromium (III) oxide is not completely removed by the hydrofluoric acidic pickling and enhances further deposition of the coating during the immersion in the chromate conversion bath.

The description of the coating deposition mechanism shows that the species responsible for the protection of the alloy are trivalent chromium compounds: $Cr(OH)_3(s)$ and $Cr_2O_3(s)$. The presence of $K_2CrO_4(s)$ or $CrO_3(s)$ trapped in the coating allows a unique 'self-healing' property of the coating.

The chromate conversion coatings are actually the reference for the protection of magnesium alloys, and their only disadvantage is the toxicity of its main compound. Alternative coatings exist and present some difference with the chromium VI process. Naturally, considering the data from the Cr(VI) coating deposition mechanism, Cr(III) could be considered as the replacement for CCC. However, less corrosion resistance is obtained with Cr(III) coatings. This is due to the deposition of a thinner layer and the absence of hexavalent species in the coating that are responsible for the 'self- healing' effect. The phosphatization of metals is a well-known process, and zinc can be added to the bath to increase the protection of magnesium to form mixed $Mg_3(PO_4)_2$ and $Zn_3(PO_4)_2$ layers. Zinc phosphate has superior corrosion resistance, but it presents no evidence of having the ability to 'self-heal'.

REE coatings could be considered as a solution, but only alloys that contain REEs could benefit from protection similar to CCCs. REEs and vanadium-based coatings possess a 'scavenger' and a 'self-healing' effect, respectively, that makes them comparable to the CCC. However, REE salts are expensive, and the efficiency of vanadium coating is highly dependent on the substrate composition.

Permanganate can be used alone or with phosphate to create an efficient protective coating made essentially by a MnO_2 layer with $Mg_3(PO_4)_2$ when phosphate has been added in the solution. The properties of the coating could also be linked to the manganese speciation in the coating: Mn (IV) and Mn (VII). Mn (VII) gives the coating a self-healing property, like the chromate conversion coatings. The protection against corrosion is also better than chromium VI coatings when optimum conditions on phosphates concentration and pH are respected. **Table 8** presents a summary of the advantages and disadvantages of each alternative solution.

Coating	Advantages	Disadvantages
CCC	Good corrosion resistance	High toxicity of its main compound
Cr(III)	Resistance to heating superior to CCC	Less corrosion resistance than CCC Thinner layer
Phosphate	Less affected by heat than CCC	Small improvement of the corrosion resistance
Zinc phosphate	Corrosion resistance equal to CCC	Problem of adhesion of the coating to the substrate
PCC (permanganate conversion coating)	No bath heating necessary, less affected by heat than CCC	Need to stabilize the pH
Permanganate/phosphate	Better corrosion resistance than CCC	Need to stabilize the pH
Vanadium	Scavenger effect	Expensive
REEs (rare earth elements–based coating)	Self-healing	Corrosion protection sensitive to alloy composition

Table 8. Summary of the advantages/disadvantages for each coating in comparison to the CCC (chromate conversion coating).

http://dx.doi.org/10.5772/66604

Such coatings mixing an oxidizing agent and a precipitating agent should be developed and tested with different combinations to optimize the alternatives to chromate conversion coatings for the protection of magnesium against corrosion. Moreover, in order to develop more efficient coatings without any chromate, it will be necessary to take into account the entire process with the pre-treatment steps and the possible interactions with the magnesium substrate. They should then be validated by tests at industrial scale.

Author details

Jérôme Frayret*, Jean Charles Dupin and Sébastien Pommiers

*Address all correspondence to: jerome.frayret@univ-pau.fr

University of Pau and Adour Countries, IRPEM, UMR, Pau, France

References

[1] B.L. Mordike, T. Ebert, Magnesium: properties — applications — potential, Materials Science and Engineering: A, 302 (2001) 37–45.

[2] R. Ferragut, F. Moia, F. Fiori, D. Lussana, G. Riontino, Small-angle X-ray scattering study of the early stages of precipitation in a Mg–Nd–Gd (EV31) alloy, Journal of Alloys and Compounds, 495 (2010) 408–411.

[3] W. Zhou, D. Shan, E.-H. Han, W. Ke, Structure and formation mechanism of phosphate conversion coating on die-cast AZ91D magnesium alloy, Corrosion Science, 50 (2008) 329–337.

[4] H. Ardelean, I. Frateur, P. Marcus, Corrosion protection of magnesium alloys by cerium, zirconium and niobium-based conversion coatings, Corrosion Science, 50 (2008) 1907–1918.

[5] M. Zhao, S. Wu, J. Luo, Y. Fukuda, H. Nakae, A chromium-free conversion coating of magnesium alloy by a phosphate–permanganate solution, Surface and Coatings Technology, 200 (2006) 5407–5412.

[6] J.E. Gray, B. Luan, Protective coatings on magnesium and its alloys — a critical review, Journal of Alloys and Compounds, 336 (2002) 88–113.

[7] C. Wang, S. Zhu, F. Jiang, F. Wang, Cerium conversion coatings for AZ91D magnesium alloy in ethanol solution and its corrosion resistance, Corrosion Science, 51 (2009) 2916–2923.

[8] M. Menta, J. Frayret, C. Gleyzes, A. Castetbon, M. Potin-Gautier, Development of an analytical method to monitor industrial degreasing and rinsing baths, Journal of Cleaner Production, 20 (2012) 161–169.

[9] S.A. Kulinich, A.S. Akhtar, D. Susac, P.C. Wong, K.C. Wong, K.A.R. Mitchell, On the growth of conversion chromate coatings on 2024-Al alloy, Applied Surface Science, 253 (2007) 3144–3153.

[10] R. Amini, A.A. Sarabi, The corrosion properties of phosphate coating on AZ31 magnesium alloy: The effect of sodium dodecyl sulfate (SDS) as an eco-friendly accelerating agent, Applied Surface Science, 257 (2011) 7134–7139.

[11] C. Askham, A.L. Gade, O.J. Hanssen, Combining REACH, environmental and economic performance indicators for strategic sustainable product development, Journal of Cleaner Production, 35 (2012) 71–78.

[12] X. Zhang, C. van den Bos, W.G. Sloof, A. Hovestad, H. Terryn, J.H.W. de Wit, Comparison of the morphology and corrosion performance of Cr(VI)- and Cr(III)-based conversion coatings on zinc, Surface and Coatings Technology, 199 (2005) 92–104.

[13] W.-K. Chen, C.-Y. Bai, C.-M. Liu, C.-S. Lin, M.-D. Ger, The effect of chromic sulfate concentration and immersion time on the structures and anticorrosive performance of the Cr(III) conversion coatings on aluminum alloys, Applied Surface Science, 256 (2010) 4924–4929.

[14] Y. Song, D. Shan, R. Chen, F. Zhang, E.-H. Han, A novel phosphate conversion film on Mg–8.8Li alloy, Surface and Coatings Technology, 203 (2009) 1107–1113.

[15] Y. Song, D. Shan, R. Chen, F. Zhang, E.-H. Han, Formation mechanism of phosphate conversion film on Mg–8.8Li alloy, Corrosion Science, 51 (2009) 62–69.

[16] N. Van Phuong, S. Moon, Comparative corrosion study of zinc phosphate and magnesium phosphate conversion coatings on AZ31 Mg alloy, Materials Letters, 122 (2014) 341–344.

[17] L.Y. Niu, Z.H. Jiang, G.Y. Li, C.D. Gu, J.S. Lian, A study and application of zinc phosphate coating on AZ91D magnesium alloy, Surface and Coatings Technology, 200 (2006) 3021–3026.

[18] G.Y. Li, J.S. Lian, L.Y. Niu, Z.H. Jiang, Q. Jiang, Growth of zinc phosphate coatings on AZ91D magnesium alloy, Surface and Coatings Technology, 201 (2006) 1814–1820.

[19] H. Umehara, M. Takaya, S. Terauchi, Chrome-free surface treatments for magnesium alloy, Surface and Coatings Technology, 169–170 (2003) 666–669.

[20] S.-Y. Jian, Y.-R. Chu, C.-S. Lin, Permanganate conversion coating on AZ31 magnesium alloys with enhanced corrosion resistance, Corrosion Science, 93 (2015) 301–309.

[21] D. Hawke, D.L. Albright, A phosphate-permanganate conversion coating for magnesium, Metal Finishing, 93 (1995) 34–38.

[22] K.Z. Chong, T.S. Shih, Conversion-coating treatment for magnesium alloys by a permanganate–phosphate solution, Materials Chemistry and Physics, 80 (2003) 191–200.

[23] Y.L. Lee, Y.R. Chu, W.C. Li, C.S. Lin, Effect of permanganate concentration on the formation and properties of phosphate/permanganate conversion coating on AZ31 magnesium alloy, Corrosion Science, 70 (2013) 74–81.

[24] K.H. Yang, M.D. Ger, W.H. Hwu, Y. Sung, Y.C. Liu, Study of vanadium-based chemical conversion coating on the corrosion resistance of magnesium alloy, Materials Chemistry and Physics, 101 (2007) 480–485.

[25] A.S. Hamdy, I. Doench, H. Möhwald, Vanadia-based coatings of self-repairing functionality for advanced magnesium Elektron ZE41 Mg–Zn–rare earth alloy, Surface and Coatings Technology, 206 (2012) 3686–3692.

[26] A.S. Hamdy, I. Doench, H. Möhwald, Smart self-healing anti-corrosion vanadia coating for magnesium alloys, Progress in Organic Coatings, 72 (2011) 387–393.

[27] A.S. Hamdy, I. Doench, H. Möhwald, Assessment of a one-step intelligent self-healing vanadia protective coatings for magnesium alloys in corrosive media, Electrochimica Acta, 56 (2011) 2493–2502.

[28] X. Jiang, R. Guo, S. Jiang, Evaluation of self-healing ability of Ce–V conversion coating on AZ31 magnesium alloy, Journal of Magnesium and Alloys, 4 (2016) 230–241.

[29] L. Li, J. Lei, S. Yu, Y. Tian, Q. Jiang, F. Pan, Formation and characterization of cerium conversion coatings on magnesium alloy, Journal of Rare Earths, 26 (2008) 383–387.

[30] L. Yang, J. Li, X. Yu, M. Zhang, X. Huang, Lanthanum-based conversion coating on Mg–8Li alloy, Applied Surface Science, 255 (2008) 2338–2341.

[31] J.F. Moulder, W.F. Stickle, P.E. Sobol, K. Bomben, Handbook of X-ray Photoelectron Spectroscopy, Perkin-Elmer Corporation (Physical Electronics), 2nd ed., 1992.

[32] T.L. Barr, The nature of the relative bonding chemistry in zeolites: an XPS study, Zeolite, 10 (1990) 760–765.

[33] H. Zhang, G. Yao, S. Wang, Y. Liu, H. Luo, A chrome-free conversion coating for magnesium–lithium alloy by a phosphate–permanganate solution, Surface and Coatings Technology, 202 (2008) 1825–1830.

[34] M. Pourbaix, Electrochemical Equilibrium Atlas at 25°C, Gauthier-Villar, 1963.

[35] R. Smith, A.E. Martell, Critical Stability Constants, Plenum Press, New York and London, 1976.

[36] W.M. Haynes, CRC Handbook of Chemistry and Physics, 83re Edn ed., CRC Press, Floride, 2013.

[37] H. Ma, Y. Berthier, P. Marcus, AES, XPS, and TDS study of the adsorption and desorption of NH_3 on ultra-thin chromium oxide films formed on chromium single crystal surfaces, Applied Surface Science, 153 (1999) 40–46.

[38] M. Oku, S. Suzuki, N. Ohtsu, T. Shishido, K. Wagatsuma, Comparison of intrinsic zero-energy loss and Shirley-type background corrected profiles of XPS spectra for quantitative surface analysis: Study of Cr, Mn and Fe oxides, Applied Surface Science, 254 (2008) 5141–5148.

[39] M. Dabalà, K. Brunelli, E. Napolitani, M. Magrini, Cerium-based chemical conversion coating on AZ63 magnesium alloy, Surface and Coatings Technology, 172 (2003) 227–232.

[40] X. Cui, Y. Yang, E. Liu, G. Jin, J. Zhong, Q. Li, Corrosion behaviors in physiological solution of cerium conversion coatings on AZ31 magnesium alloy, Applied Surface Science, 257 (2011) 9703–9709.

[41] X. Wang, L. Zhu, X. He, F. Sun, Effect of cerium additive on aluminum-based chemical conversion coating on AZ91D magnesium alloy, Applied Surface Science, 280 (2013) 467–473.

[42] L. Kouisni, M. Azzi, M. Zertoubi, F. Dalard, S. Maximovitch, Phosphate coatings on magnesium alloy AM60 part 1: study of the formation and the growth of zinc phosphate films, Surface and Coatings Technology, 185 (2004) 58–67.

[43] T.S.N.S. Narayanan, Surface pretreatment by phosphate conversion coatings—A review, Reviews on Advanced Materials Science, 9 (2005) 130–177.

[44] X.B. Chen, N. Birbilis, T.B. Abbott, Effect of [Ca^{2+}] and [] levels on the formation of calcium phosphate conversion coatings on die-cast magnesium alloy AZ91D, Corrosion Science, 55 (2012) 226–232.

[45] Y. Cheng, H. Wu, Z. Chen, H. Wang, L. Li, Phosphating process of AZ31 magnesium alloy and corrosion resistance of coatings, Transactions of Nonferrous Metals Society of China, 16 (2006) 1086–1091.

[46] N.V. Phuong, K.H. Lee, D. Chang, S. Moon, Effects of Zn^{2+} concentration and pH on the zinc phosphate conversion coatings on AZ31 magnesium alloy, Corrosion Science, 74 (2013) 314–322.

[47] L. Kouisni, M. Azzi, F. Dalard, S. Maximovitch, Phosphate coatings on magnesium alloy AM60: Part 2: electrochemical behaviour in borate buffer solution, Surface and Coatings Technology, 192 (2005) 239–246.

[48] Q. Li, S. Xu, J. Hu, S. Zhang, X. Zhong, X. Yang, The effects to the structure and electrochemical behavior of zinc phosphate conversion coatings with ethanolamine on magnesium alloy AZ91D, Electrochimica Acta, 55 (2010) 887–894.

[49] S.A. Kulinich, A.S. Akhtar, P.C. Wong, K.C. Wong, K.A.R. Mitchell, Growth of permanganate conversion coating on 2024-Al alloy, Thin Solid Films, 515 (2007) 8386–8392.

[50] C.S. Lin, C. Lee, W. Li, Y. Chen, G. Fang, Formation of phosphate/permanganate conversion coating on AZ31 magnesium alloy, Journal of The Electrochemical Society, 153 (2006) B90–B96.

[51] X.-B. Chen, X. Zhou, T.B. Abbott, M.A. Easton, N. Birbilis, Double-layered manganese phosphate conversion coating on magnesium alloy AZ91D: insights into coating formation, growth and corrosion resistance, Surface and Coatings Technology, 217 (2013) 147–155.

[52] A.S. Hamdy, I. Doench, H. Mö ;hwald, The effect of vanadia surface treatment on the corrosion inhibition characteristics of an advanced magnesium Elektron 21 alloy in chloride media, International Journal of Electrochemical Science, 7 (2012) 7751–7761.

[53] X. Yang, G. Wang, G. Dong, F. Gong, M. Zhang, Rare earth conversion coating on Mg–8.5Li alloys, Journal of Alloys and Compounds, 487 (2009) 64–68.

[54] S.-X. Yu, J.-Y. Cao, L. Chen, J. Han, R.-J. Zhang, Corrosion resistance, composition and structure of RE chemical conversion coating on magnesium alloy, Transactions of Nonferrous Metals Society of China, 18, Supplement 1 (2008) s349–s353.

[55] T. Takenaka, T. Ono, Y. Narazaki, Y. Naka, M. Kawakami, Improvement of corrosion resistance of magnesium metal by rare earth elements, Electrochimica Acta, 53 (2007) 117–121.

[56] A.L. Rudd, C.B. Breslin, F. Mansfeld, The corrosion protection afforded by rare earth conversion coatings applied to magnesium, Corrosion Science, 42 (2000) 275–288.

IntechOpen